JOURNAL OF MATERIALS SCIENCE 37 (2002) 689–697

Laser chemical vapor deposition of TiC on tantalum

M. SHANE NOEL*, D. KOVAR*,‡
*Materials Science and Engineering Program and ‡The Department of Mechanical Engineering, The University of Texas at Austin, Austin, TX 78712, USA
E-mail: dkovar@mail.utexas.edu

Laser chemical vapor deposition (LCVD) of titanium carbide (TiC) coatings onto tantalum substrates using hydrogen gas, titanium tetrachloride ($TiCl_4$) and either methane (CH_4) or acetylene (C_2H_2) source gasses was investigated. The influences of the molar ratio of the source gases and the deposition temperature on the phase assemblage, composition, and morphology of the coatings was examined. Using C_2H_2, nearly stoichiometric coatings were produced at 1000°C and at a $TiCl_4/C_2H_2$ ratio of 1/0.4. Stoichiometric coatings were also produced using CH_4 but the deposition temperature was 400°C higher and a much larger fraction of the carbon source was required compared to C_2H_2. Although deposition rates were much slower when using CH_4, the coatings exhibited a smoother surface finish and had a higher density compared to those produced using C_2H_2. The suitability of CH_4 and C_2H_2 as carbon sources for depositing stoichiometric, phase-pure coatings is discussed in light of these results.

1. Introduction

Titanium carbide (TiC) coatings are produced using chemical vapor deposition (CVD) by the cutting tool industry on a routine basis. Because of its high temperature stability, TiC has also been considered for use as an inert coating to protect substrates from reactive molten metals [1, 2]. In this application, chemical composition and stoichiometry are critical because impurities in the coatings or variations in chemical composition can lead to reactions between the coating and molten metal [3].

Processing conditions required to achieve high chemical purity and stoichiometry of TiC coatings have been studied extensively using both CVD [4–6] and laser chemical vapor deposition (LCVD) [1, 7–13]. Thermodynamic and experimental studies have been performed using carbon tetrachloride (CCl_4), methane (CH_4), and ethylene (C_2H_4) as the carbon source to predict the influence of deposition temperature and source gas concentration on TiC composition [4–7, 14]. Most of these studies have been conducted using reactive substrates such as graphite, tungsten carbide, steel or silica.

In the present study, titanium carbide coatings were deposited by LCVD onto pure tantalum substrates with the goal of producing phase-pure, stoichiometric coatings. Two reactive gas mixtures were investigated, $TiCl_4$, H_2, with CH_4 and $TiCl_4$, H_2, with acetylene (C_2H_2). Among common hydrocarbon sources, carbon is most readily dissociated from C_2H_2 and least readily from CH_4 [15]. Thus, the use of C_2H_2 could potentially reduce deposition temperatures significantly. Differences in deposition temperature, stoichiometry, quality, and quantity of the TiC deposit achieved with these carbon sources are explored.

2. Experimental

2.1. Reactor design

Deposition of the coatings was performed in a horizontal, quartz tube reactor shown schematically in Fig. 1. A 300 W, continuous wave Nd : YAG laser (Model #305, US Laser, Trent, NJ) operating at a wavelength of 1.06 μm was used as the heat source for the CVD reaction. The substrate was held upright in the reactor tube using a sample holder constructed from Al_2O_3 and BN such that the incidence of the laser was normal to the substrate surface. A diverging/converging lens combination was used to focus the beam with the substrate placed 15 mm behind the focal point. The slightly defocused beam produced a laser spot with a diameter of approximately 2 mm.

An optical pyrometer (MAS2, Raytek, Santa Cruz, CA) was used to measure the temperature of the substrate at the location of laser incidence. The pyrometer operated at a wavelength of 1.6 μm and had a target diameter of 1 mm. Since the size of the pyrometer target was finite and the laser temperature profile was Gaussian, the pyrometer reading represented an average temperature integrated over the size of the pyrometer target. A LabVIEW® (5.0, National Instruments, Austin, TX) interface was used to collect the readings from the pyrometer at an acquisition rate of 50 ms and simultaneously control the laser power in order to maintain a constant deposition temperature. With this arrangement the relative temperature control via the software PID was measured to be constant to within ±10°C.

The quartz reaction tube was mounted on a x-z table to allow for scanning of the laser beam across the entire substrate surface. The table had an intrinsic speed

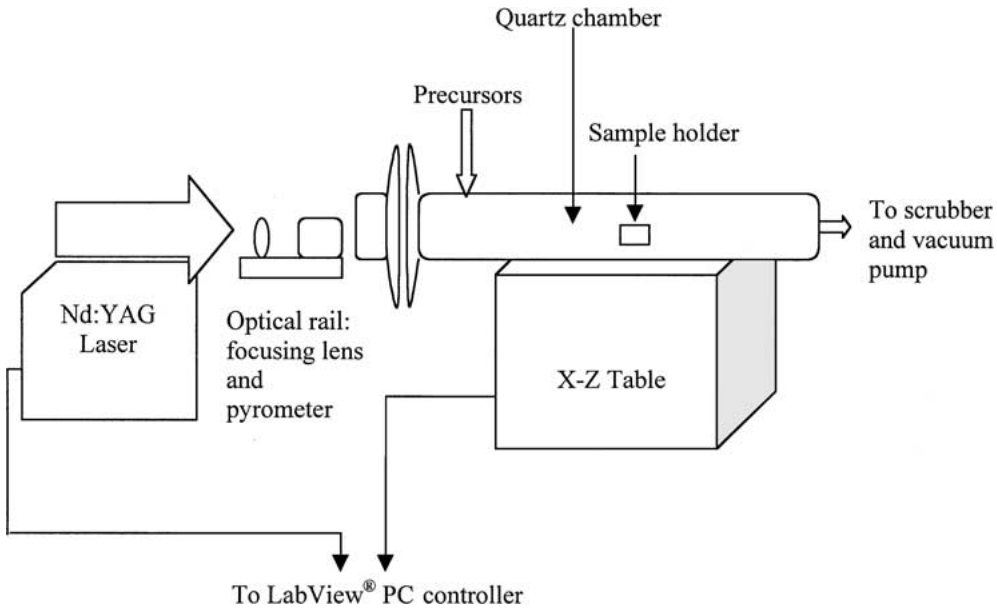

Figure 1 Schematic of LCVD system.

range of 0.4–4.0 cm/sec and a step size of 12.5 μm. A slower scan velocity was achieved by alternating single steps with pauses of 80 to 40 msec at each step. These pauses slowed the effective scan speed to between 20–100 μm/sec.

2.2. LCVD experiments

Annealed tantalum substrates (99.99%, Goodfellow, Berwyn, PA) were cut into $5 \times 7 \times 1$ mm pieces and ultrasonically cleaned in acetone prior to deposition. The Ti source for all experiments was $TiCl_4$ (99.995%, Aldrich, St. Louis, MO). Two different carbon sources were studied, ultra high purity CH_4 (99.97%, Linde, Cleveland, OH) and atomic absorption grade C_2H_2 (99.6%, Praxair, Danbury, CT). All experiments were performed under a H_2 atmosphere (99.995%, Praxair, Danbury, CT).

Prior to each experiment, the chamber was evacuated using a mechanical pump to a base pressure of 10^{-3} torr (0.133 Pa). The chamber was subsequently filled with dry argon (99.999%, Praxair, Danbury, CT) and evacuated again. This process was repeated several times in order to reduce the partial pressure of oxygen within the chamber. The precursor gases were then introduced sequentially into the reaction chamber. For all experiments, the partial pressure of $TiCl_4$ was held constant at 7 torr (930 Pa), which is the vapor pressure of $TiCl_4$ at room temperature [16]. After introduction of the $TiCl_4$, controlled amounts of the carbon precursor were added. Lastly, an appropriate amount of H_2 was added to achieve a constant total pressure. Deposition occurred at a fixed total pressure under a static gaseous atmosphere. The experimental variables that were examined included the deposition temperature, the molar ratio of $TiCl_4$/carbon source, and the type of carbon source (CH_4 or C_2H_2).

For the experiments conducted with C_2H_2, the total pressure was fixed at 200 torr (27 kPa) and the amount of C_2H_2 was varied from 3–7 torr yielding molar ratios of $TiCl_4/C_2H_2$ of 1/0.4, 1/0.6 and 1/1. The deposition temperature was varied between 1000°C–1500°C. The coatings were deposited for 6–12 minutes over an area of 35 mm^2. Thus, the laser scanned each region of the substrate 2–4 times. For the experiments conducted with CH_4 as the carbon source, the total pressure was again fixed at 200 torr (27 kPa). A $TiCl_4/CH_4$ molar ratio of 1/3 was examined at three temperatures, 1400°C, 1500°C and 1600°C. The coatings were deposited for 50 min such that the laser scanned each region of the substrate approximately 20 times.

2.3. Characterization

X-ray diffraction (XRD) was used to determine the crystalline phases present and to determine the lattice parameter of the TiC coatings. Morphological and elemental analysis was performed using a scanning electron microscope equipped with a thin-window, energy dispersive x-ray spectrometer. X-ray photoelectron spectroscopy (XPS) was utilized to determine the composition and bonding character of the coatings. The Mg Kα band (1253.6 eV) and the Al Kα band (1486.6 eV) were used as the source of x-rays for the XPS experiments. The surfaces of the films were first prepared using an Ar ion sputter for 120 seconds in order to remove surface contamination. The core binding energies for the elements Ti, C, Ta, O and Cl were then scanned.

3. Results

3.1. Deposition with C_2H_2

The theoretical threshold temperature for deposition of TiC can be calculated from the free energy change for the reaction. Based on available thermodynamic data [17], the threshold deposition temperature using C_2H_2 and $TiCl_4$ as source gasses is 548°C. Experimentally, however, significant deposition of TiC was observed only above 1000°C. At these relatively low deposition

temperatures, the deposit was strictly confined to the laser scan area where the hottest temperatures were achieved. Upon increasing the deposition temperature above 1200°C, however, a considerable amount of deposition occurred in areas outside of the laser track.

3.1.1. XRD results

X-ray diffraction patterns are shown in Fig. 2 as a function of deposition temperature for a $TiCl_4/C_2H_2$ ratio of 1/0.4. The diffraction patterns look similar for all of the temperatures that were investigated with the only crystalline phases detected being TiC and Ta. The lattice parameter for the TiC is 4.325 Å based on an average from the (111), (200), (220) and (311) diffraction peaks, consistent with a previously reported value of 4.327 Å for stoichiometric TiC [6]. Care must be taken in using this as the only evidence for stoichiometery, however, since the lattice parameter for TiC does not vary monotonically with C/Ti ratio.

X-ray diffraction patterns illustrating the influence of $TiCl_4/C_2H_2$ ratio are shown in Fig. 3 for coatings deposited at 1200°C. Again, the primary crystalline phases that are apparent are TiC and Ta. However, an additional small peak is observed at $2\theta = 38.5°$ corresponding to Ta_2C. The intensity of this diffraction peak grows as the $TiCl_4/C_2H_2$ ratio is increased. All of the coatings display a slight (220) preferred texture.

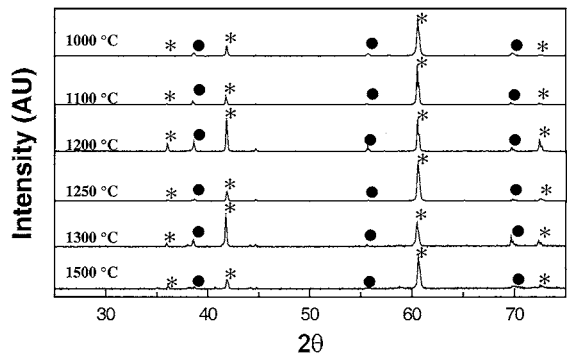

Figure 2 X-ray diffraction patterns showing the effect of deposition temperature on TiC coatings produced using C_2H_2 with a precursor ratio 1/0.4; (●) Ta, (∗) TiC.

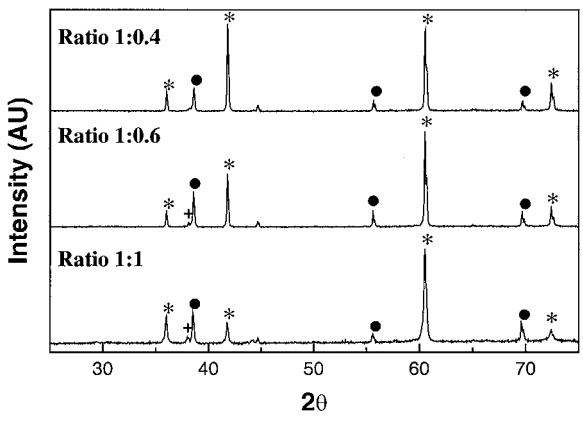

Figure 3 X-ray diffraction patterns showing the effect of the $TiCl_4/C_2H_2$ ratio on TiC coatings produced using C_2H_2 at 1200°C; (●) Ta, (∗) TiC, (+) Ta_2C.

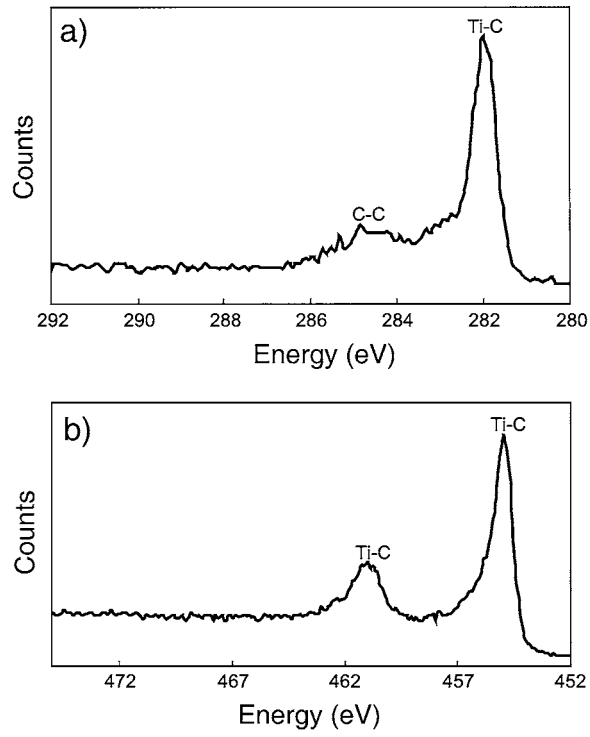

Figure 4 XPS spectra for (a) C 1s region and (b) Ti 2p region from coating produced using C_2H_2 at a deposition temperature of 1050°C using a precursor ratio of 1/0.4.

3.1.2. XPS results

XPS spectra from a typical TiC coating produced using C_2H_2 are shown in Fig. 4. The binding energy of carbon in the C-Ti bond is 282.0 eV indicating that the coating consists of TiC [18, 19]. A shoulder is also apparent on the C 1s peak shown in Fig. 4a at a binding energy of 284 eV. Similar shoulders have been reported previously in TiC over a range of energies from 283.5–285 eV that have been attributed to the presence of free carbon [18–22]. Unfortunately, the differences in the peak shifts associated with hydrocarbon contamination [19], amorphous carbon [22], or graphitic carbon [23] are usually too small to resolve and thus the form of the carbon cannot usually be differentiated from the energy of carbon shoulder alone [20, 22].

The XPS spectrum for the Ti 2p region, shown in Fig. 4b, displays the familiar $2p_{3/2}$ and $2p_{1/2}$ binding energies [24, 25], again confirming the presence of Ti-C bonding. The stoichiometry of the TiC can be assessed by comparing the peak shift relative to that of metallic Ti. For example, it has been reported that peak shifts of between +1.1–1.3 eV occur in stoichiometric TiC while smaller peak shifts indicate that the TiC is substoichiometric [18, 19]. Thus, the measured peak shifts of approximately 1.0 eV relative to Ti for both the $2p_{3/2}$ and $2p_{1/2}$ binding energies confirm that the TiC is nearly stoichiometric.

The minimal levels of oxygen that are detected are near the detection limit of about 5 at.%. There is no significant shift of the Ti peaks towards TiO_2 bonding of 458.6 eV [12], suggesting that if oxygen is present, it is substituting for carbon in the TiC lattice [26]. Chlorides were not detected with XPS indicating that significant concentrations of titanium sub-chlorides are not incorporated into the films.

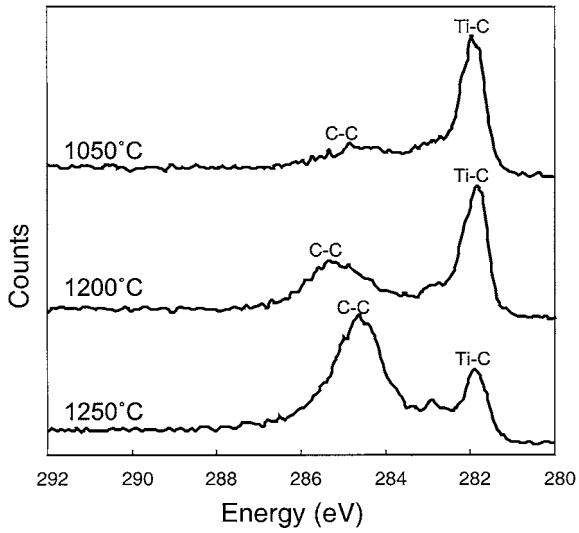

Figure 5 Evolution of the C 1s region with deposition temperature of XPS spectra for coatings produced using C_2H_2.

In Fig. 5, the evolution of the C 1s region with increasing deposition temperature is shown. At low deposition temperatures (1050°C), a small shoulder is apparent at 284 eV corresponding to C-C bonding. As the temperature is increased, the size of this shoulder increases substantially indicating that the excess carbon concentration increases with deposition temperature. The ratio of carbon to titanium in the coatings can be calculated by comparing the integrated areas of the C 1s peaks and the Ti 2p peaks. The C/(Ti + C) ratios in the coatings range from 50.2 at.% at a deposition temperature of 1050°C to 75.1 at.% carbon at 1250°C. No change in the Ti $p_{3/2}$ peak position is observed with deposition temperature indicating that the change in free carbon concentration that occurs with increasing temperature does not influence the stoichiometry of the TiC.

3.1.3. Scanning electron microscopy

In Fig. 6, a cross-sectional view of a coating that is approximately 25 μm thick is shown. This coating was deposited at 1250°C with a $TiCl_4/CH_4$ ratio of 1/0.4. From the figure, it can be seen that the coating follows the topology of the substrate and adheres to the substrate even after cross-sectional polishing. The near surface region of the coating, however, exhibits a significant amount of porosity. A very thin ($\approx$0.5 μm) interfacial layer is also apparent between the tantalum substrate and the coating.

From the EDS line-scans shown in Fig. 6, the titanium concentration is constant through the thickness of the coating except in regions where porosity is apparent. The carbon trace, in contrast, exhibits a slight gradient in concentration with the highest concentration present near the surface of the coating. Comparing the carbon, titanium, and tantalum traces, it is also apparent that the carbon concentration varies less sharply at the interface than either titanium or tantalum. The oxygen trace does not vary significantly from the substrate to the coating. This agrees with the XPS results that indicated that significant amounts of oxygen were not incorporated into the coatings.

The morphology of the coatings changes significantly with deposition temperature as shown in Fig. 7. At low temperatures (1050°C) a fairly uniform, facetted grain morphology predominates while at higher temperatures (>1300°C), a nodular morphology is apparent. A typical low temperature deposit is shown in Fig. 7a (1050°C). A dense, uniform coating is apparent

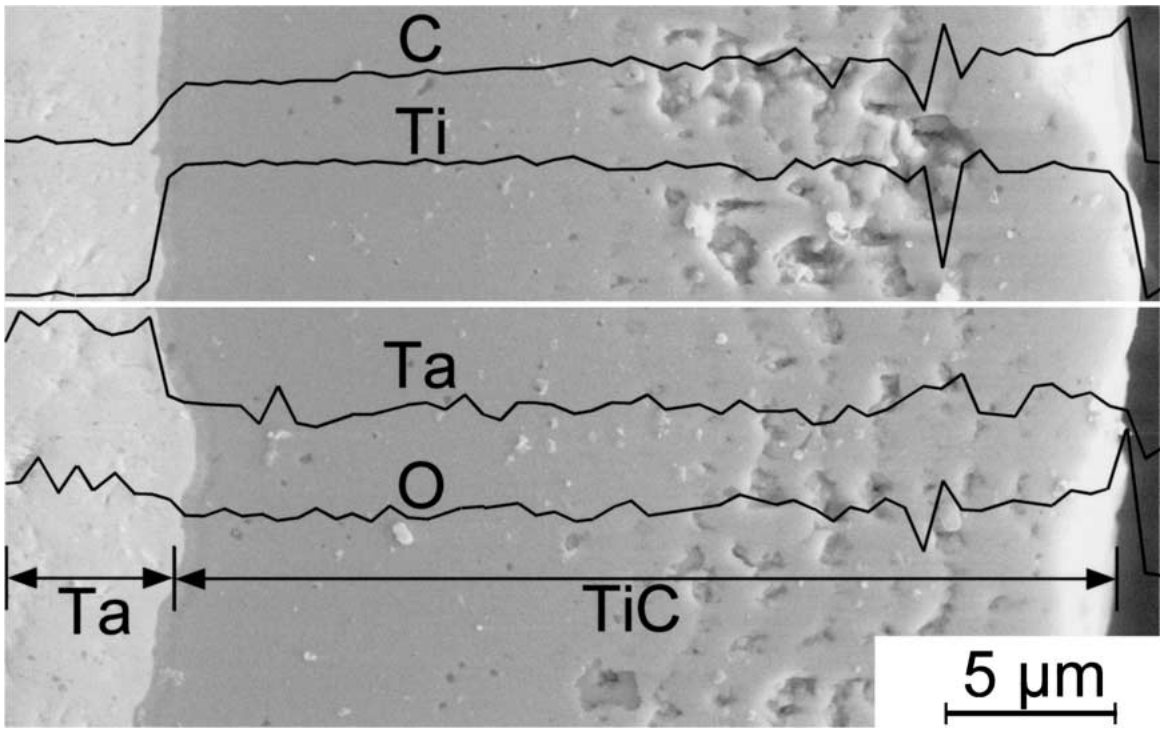

Figure 6 SEM cross-section of polished TiC coating produced using C_2H_2. Also shown are EDS line scans where the white line indicates the location of the scan.

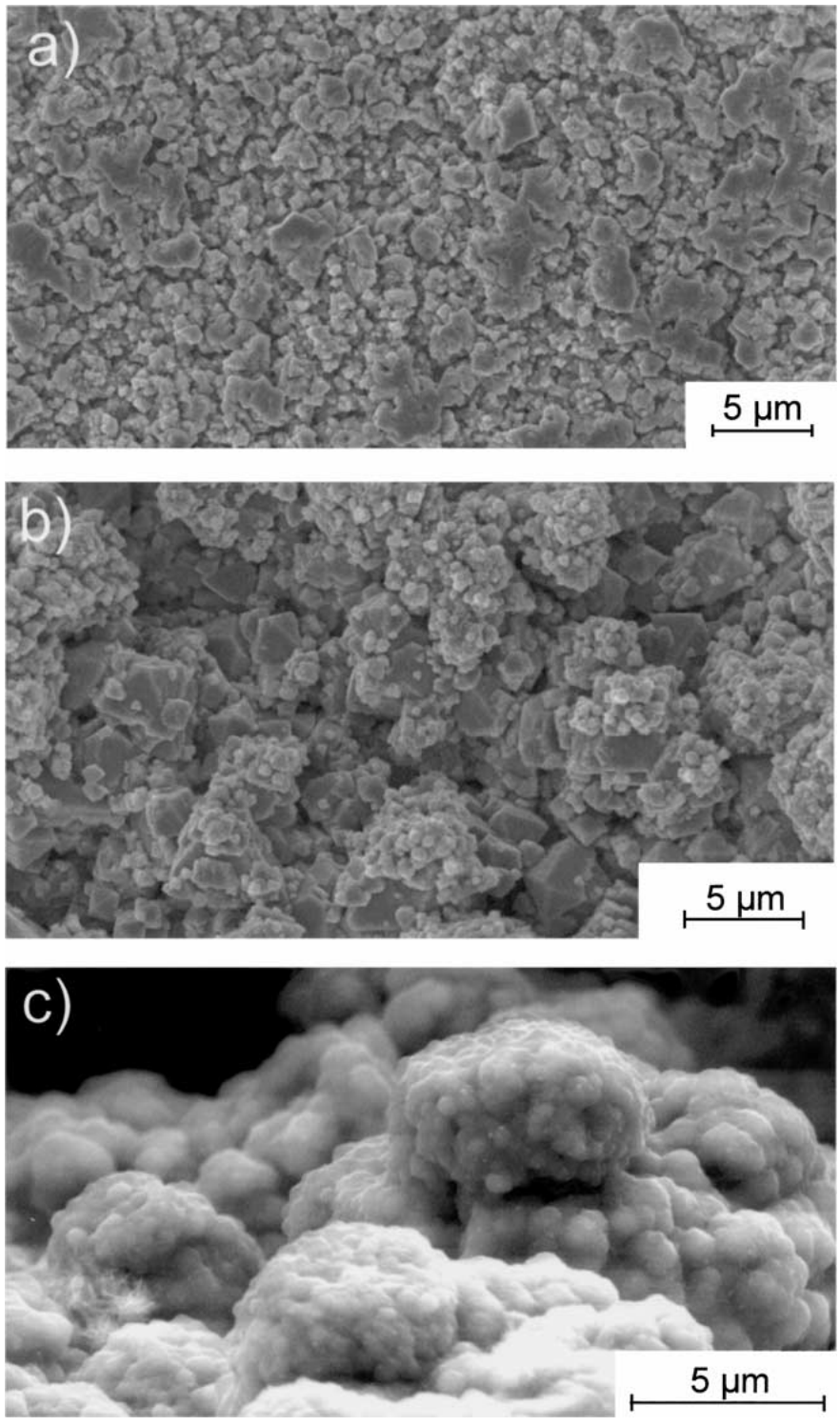

Figure 7 Plan-view SEM micrographs of TiC coatings produced using C_2H_2 at (a) 1050°C, (b) 1250°C, and (c) 1500°C.

with small facetted grains varying in size from submicron to about 2 μm. At higher deposition temperatures (Fig. 7b), considerable surface roughness develops. This coating consists of large crystallites (4 μm) covered with clusters of much smaller crystallites. At the highest deposition temperature studied (1500°C), a nodular morphology is evident with an average size greater than 5 μm. An enlarged view of a typical facetted crystallite that forms at lower deposition temperatures (<1300°C) is shown in Fig. 8. These crystallites are pyramidal and display terraces along the pyramid faces.

3.2. Deposition with CH_4

Calculations indicated that TiC formation was thermodynamically favored at temperatures above 914°C when conducted with CH_4 and $TiCl_4$. Consistent with these thermodynamic predictions, significant deposition was achieved at much higher temperatures (>1400°C) compared to C_2H_2. It was also observed that a significant amount of TiC was deposited outside of the laser path at all deposition temperatures when using CH_4. This observation suggests that heat conduction by the metallic substrate expanded the reaction zone to include much of the substrate.

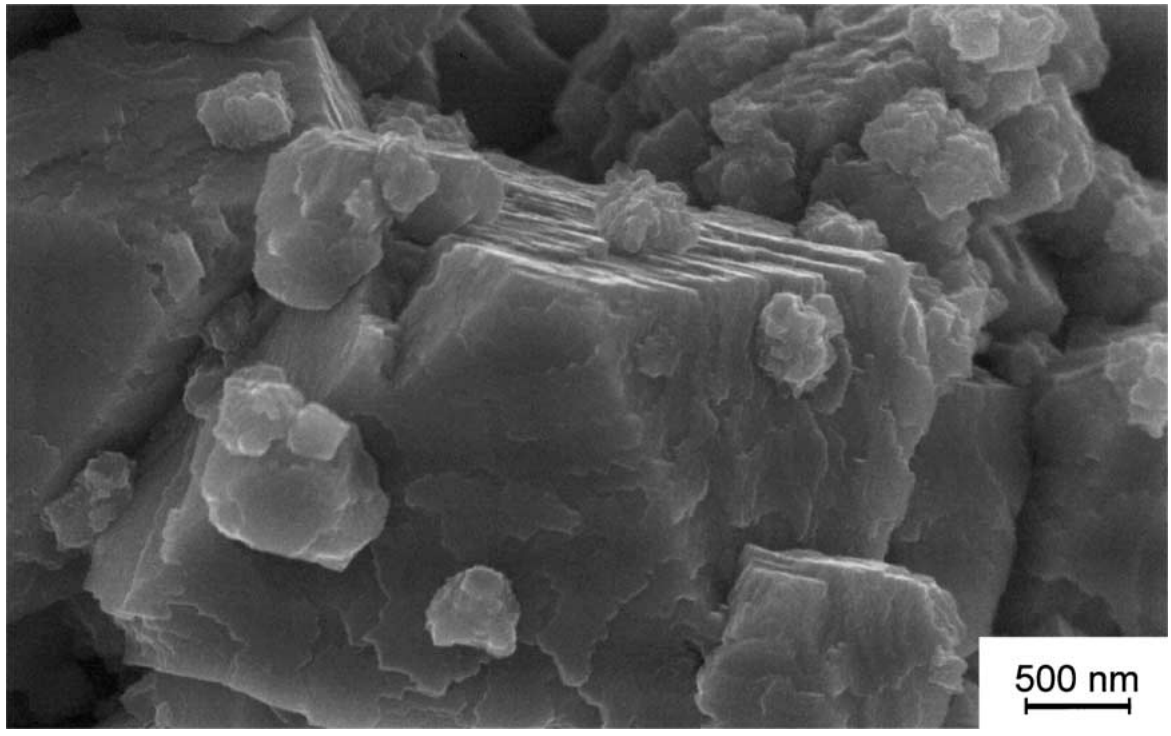

Figure 8 Typical TiC growth morphology observed for deposition from C_2H_2 at temperatures below 1250°C.

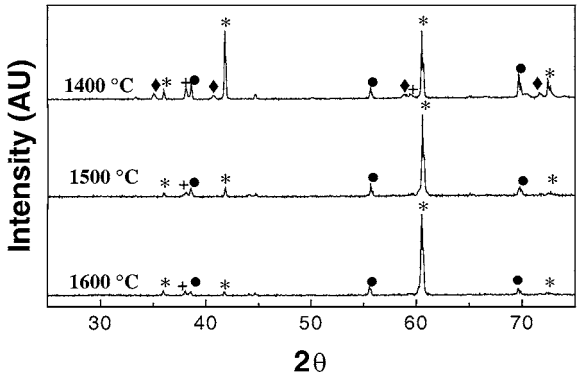

Figure 9 X-ray diffraction patterns showing the effect of deposition temperature on TiC coatings produced from CH_4; (●) Ta, (∗) TiC, (+) Ta_2C, (♦) TaC.

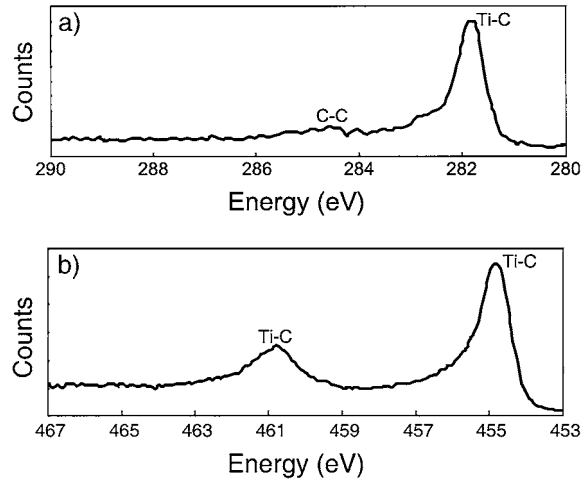

Figure 10 XPS spectra from TiC coating produced from CH_4 at 1400°C with a precursor ratio of 1/3: (a) C 1s region and (b) Ti 2p region.

3.2.1. XRD results

In Fig. 9, x-ray diffraction patterns are shown displaying the influence of temperature on phase assemblage. At 1400°C, TiC is apparent along with a small fraction of tantalum carbide phases (TaC and Ta_2C) as was the case when using C_2H_2. Also note that the (220) texture that was apparent with C_2H_2 also occurs with CH_4 and becomes more pronounced with increasing deposition temperature.

3.2.2. XPS results

XPS results from a coating produced at 1400°C using CH_4 are shown in Fig. 10. In Fig. 10a, the C 1s region displays a very slight C-C shoulder, suggesting little if any carbon co-deposition. The amount of free carbon present in the coating calculated from the area of these peaks is less than 6 at.%. The Ti 2p region has peaks at the expected Ti-C binding energies of 455 and 461 eV indicating that the TiC is nearly stoichiometric. As with the coatings produced using C_2H_2, no chlorine was detected and oxygen concentrations were near the detection limit for XPS.

3.2.3. Scanning electron microscopy

In Fig. 11, the EDS composition profile for a TiC coating produced at 1600°C using CH_4 is shown. The elemental traces are much more uniform in coatings produced from CH_4 compared to C_2H_2 (Fig. 6). A gradient in the carbon trace is again clearly evident in this figure, with the highest concentrations again present near the surface of the coating. In contrast, the titanium trace is constant throughout the coating. Tantalum and oxygen are absent as was observed in coatings produced using C_2H_2.

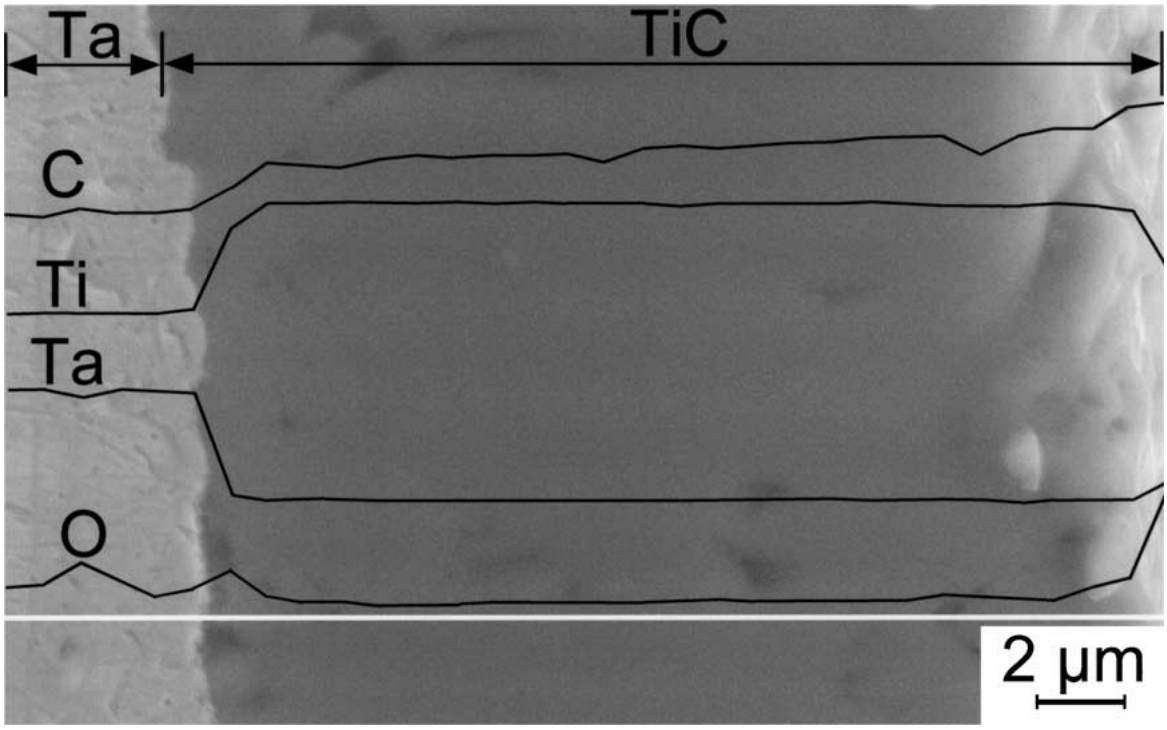

Figure 11 SEM cross-section of TiC coating produced from CH_4 showing EDS composition profile. The white line indicates location of composition scan.

Cross-sectional and plan-view micrographs of TiC coatings produced using CH_4 are shown in Fig. 12a and b, respectively. The morphology of the TiC coatings produced using CH_4 is much smoother and more uniform compared to those produced using C_2H_2 (Fig. 7). From Fig. 12b, it is apparent that the grain size is also much finer, averaging less than 1 μm.

4. Discussion

Our results indicate that it is possible to deposit nearly stoichiometric, single-phase TiC coatings free of unwanted impurities such as oxygen and chlorine using LCVD from either C_2H_2 or CH_4. Coatings with thicknesses in excess of 25 μm were produced that were free of cracks and adhered to the substrate. The critical temperature for deposition is controlled by decomposition of the hydrocarbon and, as expected from thermodynamic calculations, was about 400°C lower for C_2H_2 compared to CH_4. The differences in deposition temperatures are slightly larger than previous measurements made by conventional CVD of pyrolytic carbon using CH_4 and C_2H_2 [15].

4.1. Deposition rates

The average deposition rate using C_2H_2 calculated from SEM micrographs is 3.6 μm/min at 1250°C. In contrast, the deposition rate using CH_4 is at least 30 time slower, even at considerably higher deposition temperatures. Although direct comparisons with previous results are complicated by difficulties in accurately quantifying deposition temperature during LCVD, this deposition rate is comparable to those reported previously of 1 μm/min–10 μm/min for similar LCVD operations [1, 11, 27]. These rates are considerably faster than those reported for conventional CVD under similar processing conditions [28]. Faster deposition rates for LCVD compared to conventional CVD have been attributed to enhanced mass transport of the source gases because of convective currents around the three-dimensional hot zone [7, 29].

4.2. Phase assemblage

X-ray diffraction did not reveal the presence of graphitic carbon in any of the coatings. However, XPS revealed that carbon-carbon bonding was present in some coatings, particularly in those deposited using C_2H_2 at the highest temperatures (Figs 4 and 10). The absence of diffraction peaks for graphite combined with the XPS results showing the presence of C-C bonding confirms that any excess carbon present as a second phase is either amorphous or nanocyrstalline. The EDS results also indicated that, in samples deposited at high temperatures, the excess carbon concentration increased near the coating surface (Fig. 6). Qualitative observations indicated that at these temperatures, there was significant deposition outside of the laser track on the substrate, sample holder, and reactor walls of a substance that was most probably titanium sub-chlorides [7, 14]. Deposition of sub-chlorides on the colder regions of the substrate results in preferential depletion of the titanium source thereby increasing the fraction of carbon-containing species left in the gas phase. As a result, coatings deposited at high temperature contain a gradient in excess carbon with the highest concentration near the surface. This problem could be rectified by using a flowing gas system instead of the static system used in the current study.

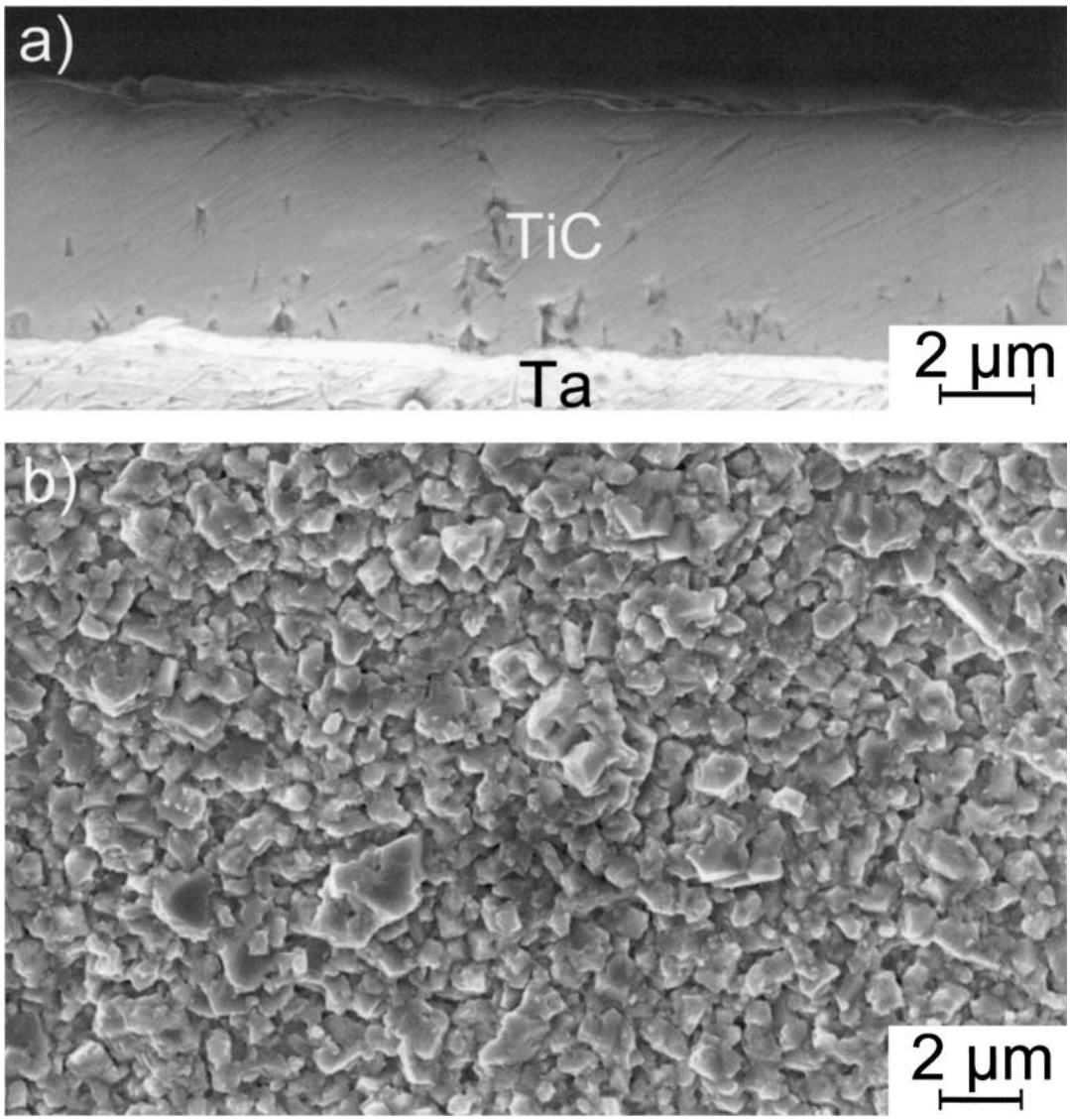

Figure 12 SEM micrographs of TiC coatings produced using CH_4: (a) cross-section and (b) plan-view.

In some of the coatings, particularly the thinner coatings, a small fraction of TaC and Ta_2C was detected using XRD (Fig. 9) and EDS (Fig. 6) as an interfacial layer between the tantalum substrate and the TiC coating. There are at least two possible explanations for this result: (1) carbon may be diffusing toward the substrate where it reacts to form tantalum carbide. (2) Tantalum is evaporating or ablating when the laser first strikes the substrate surface and is then available in the gas phase to react with carbon to form tantalum carbide. Based on the equilibrium vapor pressure of tantalum at the deposition temperature [16], sufficient evaporation of the substrate occurs when the laser first strikes the substrates to account for the observed 0.25–0.5 μm thick interfacial layer. After the initial deposition of Ta_2C or TaC (both have lower free energies of formation than TiC) onto the substrate, the source of tantalum is eliminated and TiC is subsequently deposited.

4.3. Stoichiometry of TiC

Our results indicate that it is possible to deposit nearly single-phase, stoichiometric TiC coatings using either CH_4 or C_2H_2 as carbon source gases. When using C_2H_2 as the carbon source, the carbon concentration in the coatings was found to increase when the ratio of carbon source to titanium source gas was increased. Significant increases in carbon concentration were also observed when the deposition temperature was increased. The observed influence of the ratio of source gases is expected from simple thermodynamic arguments [6]. However, there are conflicting reports in the literature with regard to the influence of deposition temperature on carbon concentration in TiC coatings. For example, Goto *et al*. have reported that carbon concentration decreases with increasing temperature when CCl_4 is used as the carbon source during conventional CVD onto graphite [6] whereas Konyashin has reported that the carbon concentration in the coatings initially decreases with increasing temperature at low temperatures and then increases at high temperatures [30]. Westberg also reported a decrease in carbon concentration with increasing temperature during LCVD using CH_4 as the carbon source [7]. These studies were conducted using graphite or WC substrates that act as a source of carbon at temperatures below that which hydrocarbon decomposition occurs. Depletion of available carbon from the substrate as coating thickness increases can

lead to decreases in carbon concentration with increasing coating thickness if an additional source of carbon in not available. If the temperature is increased so that hydrocarbon decomposition is possible, further increases in temperature should result in increases in the carbon concentration in the coatings because of the enhanced availability of carbon [4]. Our experimental findings are consistent with this prediction.

4.4. Growth morphologies

Our results show that deposition occurs with a (220) preferred texture when either CH_4 or C_2H_2 are used as source gases. Similar observations of preferred growth orientations have been reported previously for conventional CVD [31, 32] and LCVD of TiC [10, 33]. For example, TiC produced using LCVD with CH_4 as the carbon source has been shown previously to display a (200) preferred orientation at low $TiCl_4/CH_4$ ratios (1/1) and a (220) preferred orientation at higher ratios (1/7) [10].

5. Conclusions

Titanium carbide coatings deposited on tantalum substrates were produced using the LCVD technique. Two different carbon sources were studied and the variation in gas mixture and deposition temperature was demonstrated to have significant effects on the composition, phase assemblage, deposition rates, and morphology of the coatings. When C_2H_2 was used as the carbon source, a small fraction of amorphous carbon was co-deposited with stoichiometric TiC even at relatively low deposition temperatures. As the deposition temperature was increased, the fraction of excess carbon in the coatings increased substantially, as predicted from thermodynamic calculations. The grain morphology in the coatings consisted of facetted (220) oriented grains at low temperatures (<1250°C) whereas a nodular morphology was observed at higher temperatures.

When CH_4 was used as the carbon source, more uniform coatings with higher density were achieved compared to those produced using C_2H_2. These coatings were stoichiometric and nearly free of excess carbon even at high deposition temperatures. The coatings deposited with CH_4 required much higher temperatures and had much slower deposition rates compared to those produced using C_2H_2, however.

Acknowledgements

Support for this research was provided by Los Alamos National Laboratory under contract#14904-00-23. The authors would like to thank Mr. Jesus Jose Gallegos III (UT-Austin) and Dr. David Kolman (Los Alamos National Laboratory) for their insightful comments and Dr. J. Steven Swinnea (UT-Austin) for experimental assistance.

References

1. V. HOPFE, A. TEHEL, A. BAIER and J. SCHARSIG, *Appl. Surf. Sci.* **54** (1992) 78.
2. A. HATZIAPOSTOLOU, I. ZERGIOTI, E. HONTZOPOULOS, A. ZERVAKI and G. HAIDEMENOPOULOS, in "Laser Processing: Surface Treatment and Film Deposition," edited by J. Mazumder, O. Conde, R. Vilar and W. Steen (Kluwer Academic, Dordrecht, 1996) p. 703.
3. J. V. NAIDICH, V. S. ZHURAVLJOV and N. I. FRUMINA, *J. Mater. Sci.* **25** (1990) 1895.
4. F. TEYSSANDIER, C. BERNARD and M. DUCARRIOR, *J. Electrochem. Soc.* **135** (1988) 225.
5. F. TEYSSANDIER, M. DUCARROIR and C. BERNARD, *J. Less Common Met.* **78** (1981) 269.
6. T. GOTO, C.-C. JIANG and T. HIRAI, *ibid.* **159** (1990) 231.
7. H. WESTBERG, M. BOMAN and J.-O. CARLSSON, *Thin Solid Films* **218** (1992) 8.
8. H. WESTBERG, M. BOMAN, A.-S. NOREKRANS and J.-O. CARLSSON, *ibid.* **215** (1992) 126.
9. L. X. CAO *et al.*, *ibid.* **257** (1995) 7.
10. M. L. F. PARAMÊS and O. CONDE, *Applied Surface Science* **109/110** (1997) 554.
11. I. ZERGIOTI, A. ZERVAKI, A. HATZIAPOSTOLOU, G. HAIDEMENOPOULOS and E. HONTZOPOULOS, *Opt. Quantum Electron.* **27** (1995) 1377.
12. R. ALEXANDRESCU *et al.*, in "Proceedings of SPIE," edited by V. I. Vlad (International Society for Optical Engineering, Belingham, 1995) Vol. 2464, p. 103.
13. M. BOMAN and J.-O. CARLSSON, *Surf. Coat. Technol.* **49** (1991) 221.
14. F. TEYSSANDIER and M. D. ALLENDORF, *J. Electrochem. Soc.* **145** (1998) 2167.
15. P. A. TESNER, in "Chemistry and Physics of Carbon," edited by P. A. Thrower (Marcel Dekker, New York, 1984) Vol. 19, p. 65.
16. C. L. YAWS, S. NIJHAWAN and L. BU, in "Handbook of Vapor Pressure" (Gulf Publishing , Houston, 1994).
17. M. W. CHASE, in "JANAF Thermochemical Tables," 2nd ed. (American Chemical Society, Washington, D.C., 1986).
18. L. RAMQVIST, K. HAMRIN, G. JOHANSSON, A. FAHLMAN and C. NORDLING, *J. Phys. Chem. Solids* **30** (1969) 1835.
19. H. IHARA, Y. KUMASHIRO, A. ITOH and K. MAEDA, *Jpn. J. Appl. Phys.* **12** (1973) 1462.
20. M. GUEMMA, *et al.*, *Nucl. Instrum. Methods Phys. Res.* **111** (1996) 263.
21. L. ZHANG and R. V. KOKA, *Mater. Chem. Phys.* **57** (1998) 23.
22. J. HRBEK, *J. Vac. Sci. Technol.* **A4** (1986) 86.
23. B. J. BACHMAN and M. J. VASILE, *ibid.* **A7** (1989) 2709.
24. A. ERMOLIEFF, P. BERNARD, S. MARTHON and P. WITTMER, *Surf. Interface Anal.* **11** (1988) 563.
25. C. E. MYERS, H. F. FRANZEN and J. W. ANDEREGG, *Inorg. Chem.* **24** (1985) 1822.
26. J. E. KRZANOWSKI and R. E. LEUCHNER, *J. Amer. Ceram. Soc.* **80** (1997) 1277.
27. M. L. F. PARAMÊS and O. CONDE, *Journal De Physique* **3** (1993) 217.
28. J. ECHIGOYA, Z.-T. LIU, A. IMAMURA and S. TAKATSU, *Thin Solid Films* **198** (1991) 293.
29. M. S. SHAARAWI, J. M. SANCHEZ, H. KAN and A. MANTHIRAM, *J. Amer. Ceram. Soc* **83** (2000) 1947.
30. I. Y. KONYASHIN, *Thin Solid Films* **278** (1996) 37.
31. C.-C. JIANG, T. GOTO and T. HIRAI, *J. Mater. Sci.* **25** (1990) 1086.
32. S. EROGLU and B. GALLOIS, *ibid.* **30** (1995) 1754.
33. O. CONDE, A. J. SILVESTRE and M. L. PARAMÊS, in "Laser Processing: Surface Treatment and Film Deposition," edited by J. Mazumder, O. Conde, R. Vilar and W. Steen (Kluwer Academic Publishers, Dordrecht, 1996) Vol. 307, p. 665.

Received 19 April
and accepted 16 October 2001